Supplemental Materials and Methods

Human cell adhesion assays

Cell-based adhesion assays using human cell line K562 cells stably transfected with integrin CD11b/CD18 (K562 CD11b/CD18) (*54*) and immobilized human fibrinogen (Fg) as ligand were performed as previously described (*16*). Cell lines were tested and determined to be mycoplasma free. Briefly, 384-well Highbind microtiter plates were coated with 30 uL solution of human fibrinogen (15ug/ml) in Phosphate Buffered Saline (PBS), pH 7.4 containing 1mM each of Ca^{2+} and Mg^{2+} ions (PBS^{++}) overnight at 4°C overnight. To measure total input cell number, additional wells were coated with CD11b heterodimer-specific mAb IB4 (20ug/ml). Subsequently, the non-specific sites in the wells were blocked by incubation with 1% non-fat milk in Tris Buffered Saline (TBS), pH 7.4, at room temperature for 1h and subsequently washed three times with TBS. Human cells were suspended in the assay buffer (TBS containing 1mM each of Ca^{2+} and Mg^{2+} ions (TBS^{++})) and were transferred to the ligand-coated wells (30,000 cells/well). A stock solution of ADH503 was prepared in water at a concentration of 10 mM. Adhesion of K562 CD11b/CD18 cells to fibrinogen was performed for 30 min at 37°C. To dislodge non-adherent cells, the assay plates were gently inverted and kept in the inverted position for 30min at room temperature. Cells remaining adherent were fixed using formaldehyde and were quantitated using imaging microscopy, as previously described (*55*). For the blocking assays, cells were incubated with blocking mAb IB4 (20ug/ml) for 30 min at RT prior to adding them to the assay wells. Assays were performed in 4-8 replicate wells. Data shown are from one of at least two independent experiments.

Mouse cell adhesion assays

Cell adhesion assays using primary mouse macrophages were performed similar to the human cell assays above, except that the assays utilized peritoneal macrophages (isolated from C57BL/6J (B6) wild type mice ((#000664, The Jackson Laboratory), as described previously (*54*) and used mouse fibrinogen (15ug/ml) as an immobilized CD11b ligand. Additionally, anti-mouse CD11b antibody M1/70 was used for blocking assays. Assays were performed in 4-8 replicate wells. Data shown are from one of at least two independent experiments.

Assessment of ADH503 toxicity in rats and dogs.

Sprague-Dawley rats (7-8 weeks of age, 6/sex/group) were orally administered vehicle (0.5% methylcellulose containing 0.1% Tween 80 in purified water) or ADH503 (1000 mg/kg/day, administered BID) daily for 14 consecutive days. Animals were monitored for clinical signs, changes in body weight and food consumption, effects on hematological parameters and macroscopic and microscopic

changes. Blood was collected for CBC analyses. In some studies, ADH503 was administered by oral gavage to male and female Sprague-Dawley rats (n=5/sex) at 1500 mg/kg/day for 28 consecutive days. The compound was also administered by oral gavage to male and female Beagle dogs (n=3/sex) at 1359 mg/kg/day for 28 consecutive days. The daily doses were administered in three equal increments (TID) with approximately 8 hours between the doses. Separate groups of male and female animals received vehicle alone, also given TID. Animals were observed for tolerability, adverse effects, clinical signs or toxicity during this period and none were observed.

Pharmacokinetics

To evaluate the pharmacokinetics after oral administration of ADH503, Sprague-Dawley rats or C57BL/6J mice were used. ADH503 was administered at a single or multiple doses of 30-1000 mg/kg in vehicle (Tween-80 (0.02%) and 0.5% methyl cellulose in water). All animals were fasted overnight prior to dosing and through two hours postdose. Water was provided *ad libitum*. Plasma was collected at time intervals 0.25, 0.5, 1, 2, 4, 8, 10, 24, and 48 hours post-dosing. A model-independent method (Phoenix WinNonlin) was used to determine pharmacokinetic parameters for ADH503 from plasma concentration-time data.

Image analysis

For all image analysis, whole slide tissues were scans were obtained at 10X or 20X magnification on Zeiss Axio Scan Z1 Brightfield/Fluorescence Slide Scanner. Additional 20X brightfield images were taken on the Nikon Eclipse 80i Epifluorescence microscope (Nikon). Whole tissue slide scans were analyzed with HALO software (Indica Labs Perkin Elmer) using Area quantification V1.0, Cytonuclear v1.5, Cytonuclear FL v1.4 module or “Immune Cell Proximity v1.2” module. Distances less than or equal to zero were culled for clarity. Finally, the normalized percentage of CD8 T cells proximal to cytokeratin 19-expressing tumor lesions was binned and quantified.

Fluorescence-activated cell sorting

Normal or tumor-bearing mice were perfused with 20 mL of heparin-containing PBS. Tissues were digested in 25 mL of DMEM containing 2 mg/mL of collagenase A (Roche) and 1X DNase I (Sigma) for 30 minutes at 37˚C with constant stirring. $CD45^+$ cells were enriched from single cell suspensions through MACS magnetic selection using anti-mouse CD45 microbeads (Miltenyi). Elutes were blocked with rat anti-mouse CD16/CD32 antibodies (eBioscience) (1/200) for 10 minutes, pelleted by centrifugation, and labeled with fluorophore-conjugated anti-mouse antibodies at recommended dilutions for 20 minutes on ice. Cells were filtered through 40 μm Nylon mesh, and immediately sorted using Aria-II (BD Biosciences). For microarray analyses and gene expression analyses, cells were

sorted directly into RNA lysis buffer (Omega Biotek); RNA was isolated using the EZNA kit (Omega Biotek) according to instructions by the manufacturer. For *ex vivo* assays, cells were sorted into DMEM containing 20% FBS before being pelleted and resuspended for subsequent treatments.

Quantitative reverse transcription-polymerase chain reaction (Q-PCR)

Total RNA was extracted from bone marrow-derived macrophages (BM-MACs) using an E.Z.N.A. Total RNA Kit (OMEGA). cDNAs were synthesized using qScript cDNA SuperMix (QuantaBio). Quantitative real-time PCR Taqman primer probe sets specific for ARG1, YM1 and CCL2 (Applied Biosystems) were used, and the relative gene expression was determined on an ABI 7900HT quantitative PCR machine (ABI Biosystems) using Taqman Gene Expression Master Mix (Applied Biosystems). The comparative threshold cycle method was used to calculate fold changes in gene expression, which were normalized to the expression of TBP and/or GAPDH as reference genes.

Isolation of BM-MACs

BM-MACs were isolated following the protocol described previously (*7*). Marrow cells were isolated by flushing femurs and tibias from C57BL/6J mice and cultured in RPMI-1640 medium (Gibco) containing 10% FBS and 20 ng/mL macrophage colony–stimulating factor (M-CSF, PeproTech) on plastic petri plates. After 7 days in culture, adherent macrophages were harvested for co-culture experiments. Macrophages were pretreated with ADH-503 and then co-cultured with TCM for 7 hours prior to RNA isolation.

Cell proliferation assay

Cell proliferation assay was performed by using CellTiter96 Non-Radioactive Cell Proliferation Assay (Promega) according to manufacturers' instructions. Briefly, 5,000 cells/well were seeded into 96-well plates coated with 7.5 mg/mL Cultrex BME (Trevigen). At desired time points, Dye Solution was added to live cultures for 4 h at 37 °C. Absorbance was measured at 570 nm on Multiskan GO plate reader (Thermo Fisher Scientific).

Figure S1.

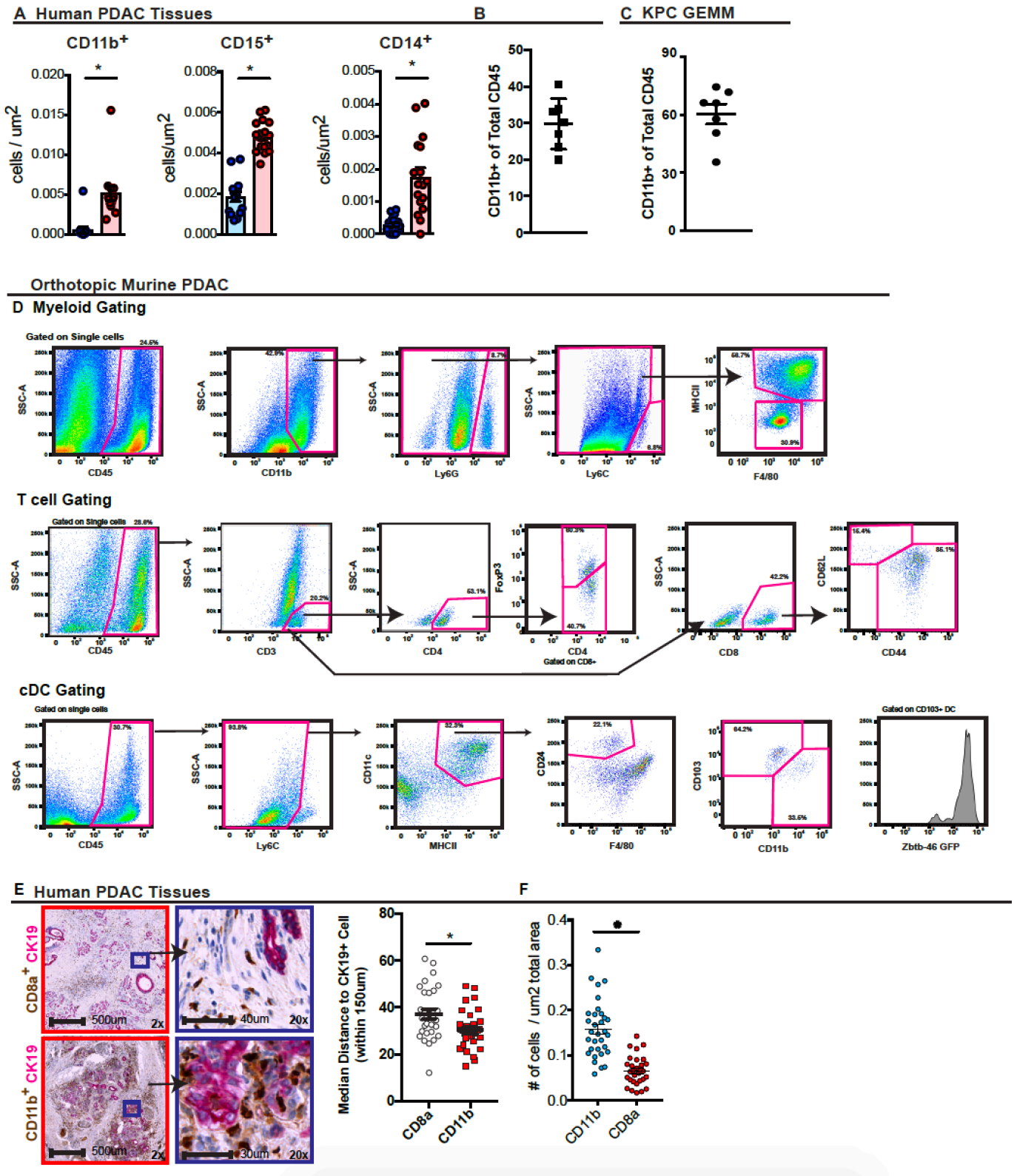
A Human PDAC Tissues
CD11b+
CD15+
CD14+
cells / um2
cells/um2
B
CD11b+ of Total CD45
C KPC GEMM
CD11b+ of Total CD45
Orthotopic Murine PDAC
D Myeloid Gating
Gated on Single cells
SSC-A
CD45
CD11b
Ly6G
Ly6C
MHCII
F4/80
T cell Gating
CD3
CD4
FoxP3
Gated on CD8+
CD8
CD62L
CD44
cDC Gating
Gated on single cells
CD11c
CD24
CD103
Gated on CD103+ DC
Zbtb-46 GFP
E Human PDAC Tissues
CD8a+ CK19
CD11b+ CK19
500um
2x
40um
20x
30um
Median Distance to CK19+ Cell (within 150um)
CD8a
CD11b
F
# of cells / um2 total area

Supplementary Figure Legends

Supplementary Fig. 1. Pancreatic ductal adenocarcinoma has a dense CD11b$^+$ myeloid infiltrate.

A) IHC analysis of human PDAC and adjacent normal tissue assessed for CD11b$^+$, CD15$^+$ and CD14$^+$ cells. Graphs show quantification of the cells (n=13 paired samples).

B) CD11b expression CyTOF analysis of human PDAC tissue samples. Graph depicts CD11b+ as a fraction of total CD45+ cells. Each dot represents an individual PDAC patient sample (n=7).

C) CD11b expression analysis of murine PDAC tissues. Graph depicts data from PDAC tissues of end stage KPC mice expressed as CD11b+ as a fraction of total leukocytes (n=7 mice).

D) Representative flow cytometry gating strategies for myeloid, T cell, and cDC identification. Data are from orthotopic KP2 PDAC model. Histogram also depicts the GFP expression in CD103$^+$ cDC1s using the Zbtb-GFP reporter mice to verify cDC identify.

E-F) Leukocyte proximity analysis. E) Representative images of CD8a or CD11b (brown) co-staining with CK19 (pink). Mean distance (E) or number (F) of CD11b+ or CD8a+ cells are depicted for areas within 150um of CK19+ tumor cells. (n=23 PDAC samples)

Graphs depicted as mean +/- standard error; * denotes $p< 0.05$ by two-sided t-test or Mann-Whitney test depending on the data distribution.

Figure S2

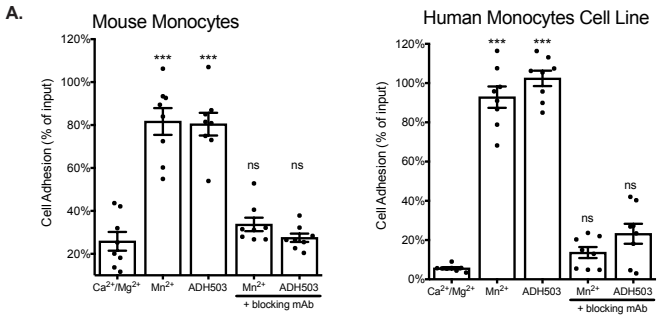

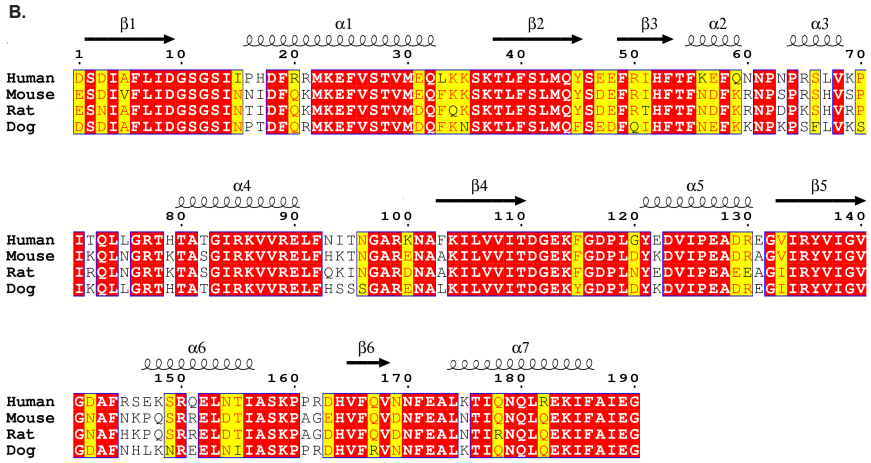

C.

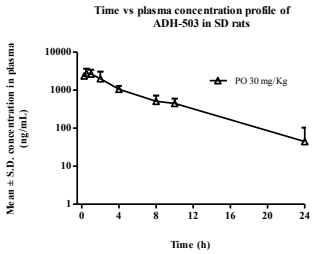

Parameter	Animal Number 1	2	3	4	Mean	S.D	%CV
$t_{1/2, \beta}$ (h)	2.84	2.94	6.38	3.20	3.84	1.70	44.2
AUC_{0-24} (ng*h/mL)	15236	12826	18898	14032	15248	2624	17.2
$AUC_{0-\infty}$ (ng*h/mL)	15305	12887	20118	14097	15602	3169	20.3
C_{max} (ng/mL)	2026	2823	3927	2700	2869	788	27.5
t_{max} (h)	0.25	0.50	0.50	1.00	0.56	0.31	55.9

D.

30 mg/Kg

Parameter	Day 1 Mean	S.D	%CV	Day 5 Mean	S.D	%CV
$t_{1/2, \beta (h)}$	4.68	0.92	19.7	9.54	11.0	115
AUC_{0-24} (ng*h/mL)	6817	1478	21.7	5952	2716	45.6
$AUC_{0-\infty}$ (ng*h/mL)	6950	1498	21.6	8206	3853	47.0
C_{max} (ng/mL)	1716	499	29.1	1900	574	30.2
t_{max} (h)	0.31	0.13	40.0	0.75	0.29	38.5

E.

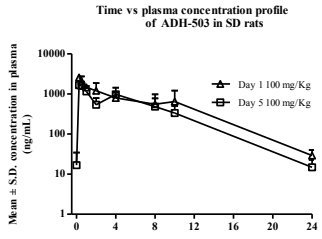

100 mg/Kg

Parameter	Day 1 Mean	S.D	%CV	Day 5 Mean	S.D	%CV
$t_{1/2, \beta (h)}$	3.95	0.71	18.0	3.48	0.98	28.2
AUC_{0-24} (ng*h/mL)	13804	5577	40.4	9512	3776	39.7
$AUC_{0-\infty}$ (ng*h/mL)	13962	5588	40.0	9840	3336	33.9
C_{max} (ng/mL)	2594	421	16.2	1800	325	18.1
t_{max} (h)	0.31	0.13	40.0	0.38	0.14	38.5

F.

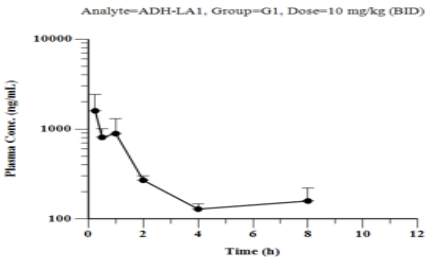

G.

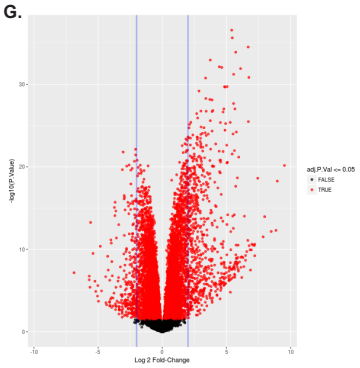

Supplementary Fig. 2: ADH-503 in-vivo properties.

A) A bar graph showing relative adhesion of peritoneal mouse macrophages or human K562 cells CD11b/CD18 to immobilized CD11b ligand mouse fibrinogen (15 μg/mL) in the presence of Ca^{2+} and Mg^{2+} ions (physiologic, low-affinity control conditions, 1 mM each), Mn^{2+} (known non-selective integrin agonist, 1 mM), or ADH-503 (20 μM), or the agonists Mn^{2+} (1mM) or ADH-503 (20 μM) in the presence of blocking anti-CD11b antibody (M1/70 or 1B4).

B) Protein sequence alignment for αA-domain of CD11b from human, mouse, rat, and dog.

C) Time vs. plasma concentration following oral administration of ADH503 to female rats. Average plasma concentration is depicted in graph (n=4 rats/group). Table depicts values for the same data set.

D) Plasma concentration-time data following oral gavage administration of ADH503 at 30 mg/kg in male rats on Day 1 and Day 5. Table is based on data displayed in graphical form in Figure 2C

E) Plasma concentration-time data following oral gavage administration of ADH503 at 100 mg/kg in male rats on Day 1 and Day 5. Table depicts values for the same data set. n=?

F) Plasma concentration-time data following oral gavage administration of ADH503 at 10 mg/kg in female mice. n=4/group

G) Vocano plot of RNA-Seq expression data on mouse bone marrow derived macrophages treated with PDAC conditioned media +/- ADH-503 for 7 hours. n=3/group

Data shown are Mean ± the standard error of mean (SEM) from at least two independent experiments (*P<0.001, ns= not significant, Student's t-test).

Figure S3.

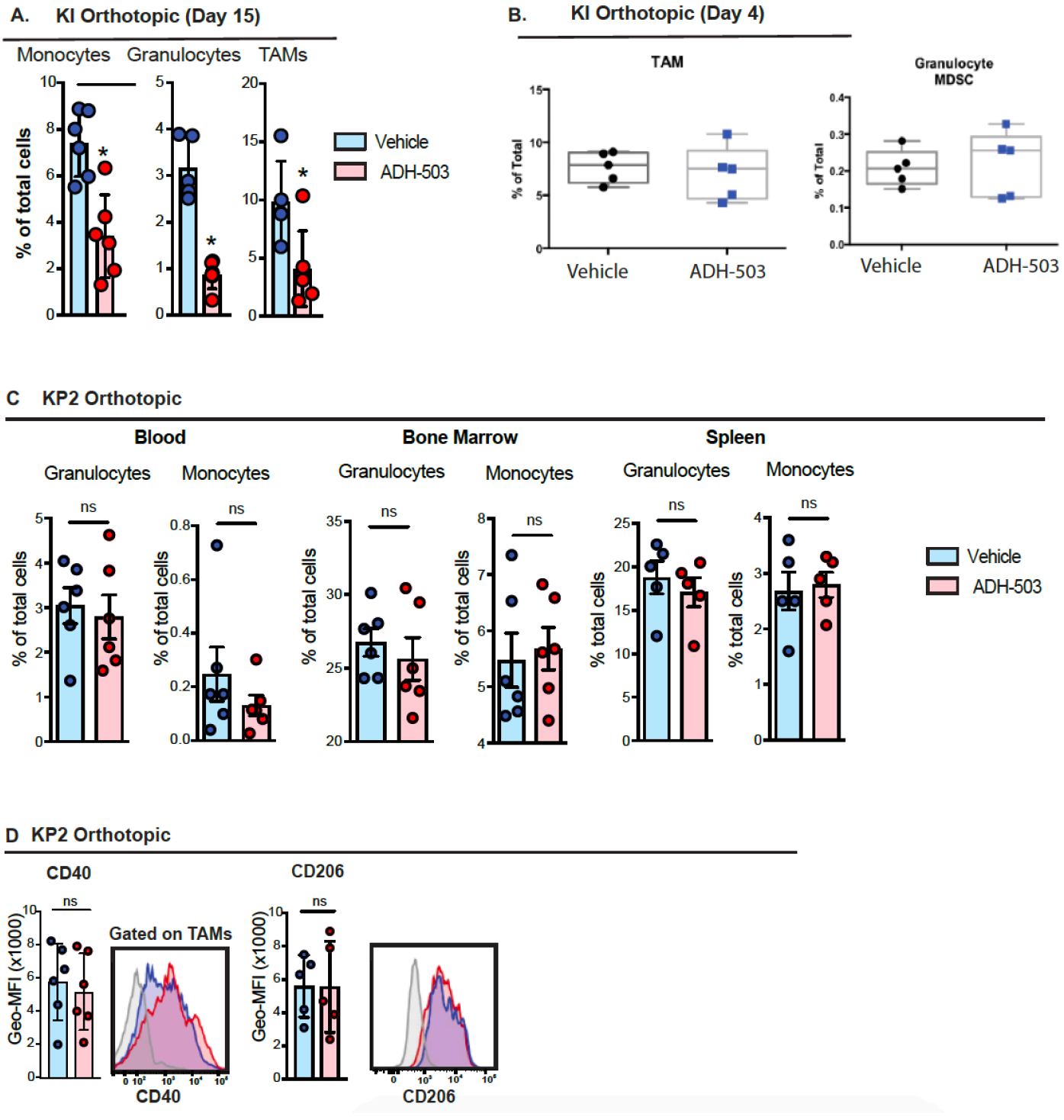
A. KI Orthotopic (Day 15)
Monocytes
Granulocytes
TAMs
% of total cells
Vehicle
ADH-503
B. KI Orthotopic (Day 4)
TAM
Granulocyte MDSC
% of Total
Vehicle
ADH-503
C KP2 Orthotopic
Blood
Bone Marrow
Spleen
Granulocytes
Monocytes
% of total cells
% total cells
ns
Vehicle
ADH-503
D KP2 Orthotopic
CD40
CD206
Geo-MFI (x1000)
Gated on TAMs
CD40
CD206

Supplementary Fig. 3: ADH-503 alters innate responses in PDAC tissues.

A) Frequency of tumor infiltrating granulocyte, monocyte, and macrophage populations in orthotopic KI PDAC tissues, after 15 days of treatment with ADH-503 or vehicle (n=6/ group).

B) Frequency of tumor infiltrating granulocytes and macrophages in orthotopic KI PDAC tissues, after 4 days of treatment with ADH-503 or vehicle (n=5/group).

C) Flow cytometry analysis of monocyte and granulocyte frequency in blood, bone marrow, and spleen of KP2 tumor-bearing mice treated with vehicle or ADH-503 for 10 days.

D) Flow cytometry analysis CD40 and CD206 on TAMs. Data depicted as histograms and geometric-mean fluorescent intensity (GEO-MFI) data on TAMs in orthotopic KP2 PDAC tissues from mice treated with ADH-503 or vehicle.

Graphs show the mean ± standard error; * denotes $P < 0.05$ by two-sided *t* test or Mann-Whitney test, depending on the data distribution. All flow cytometry data are representative of at least 2 independent in vivo experiments.

Figure S4.

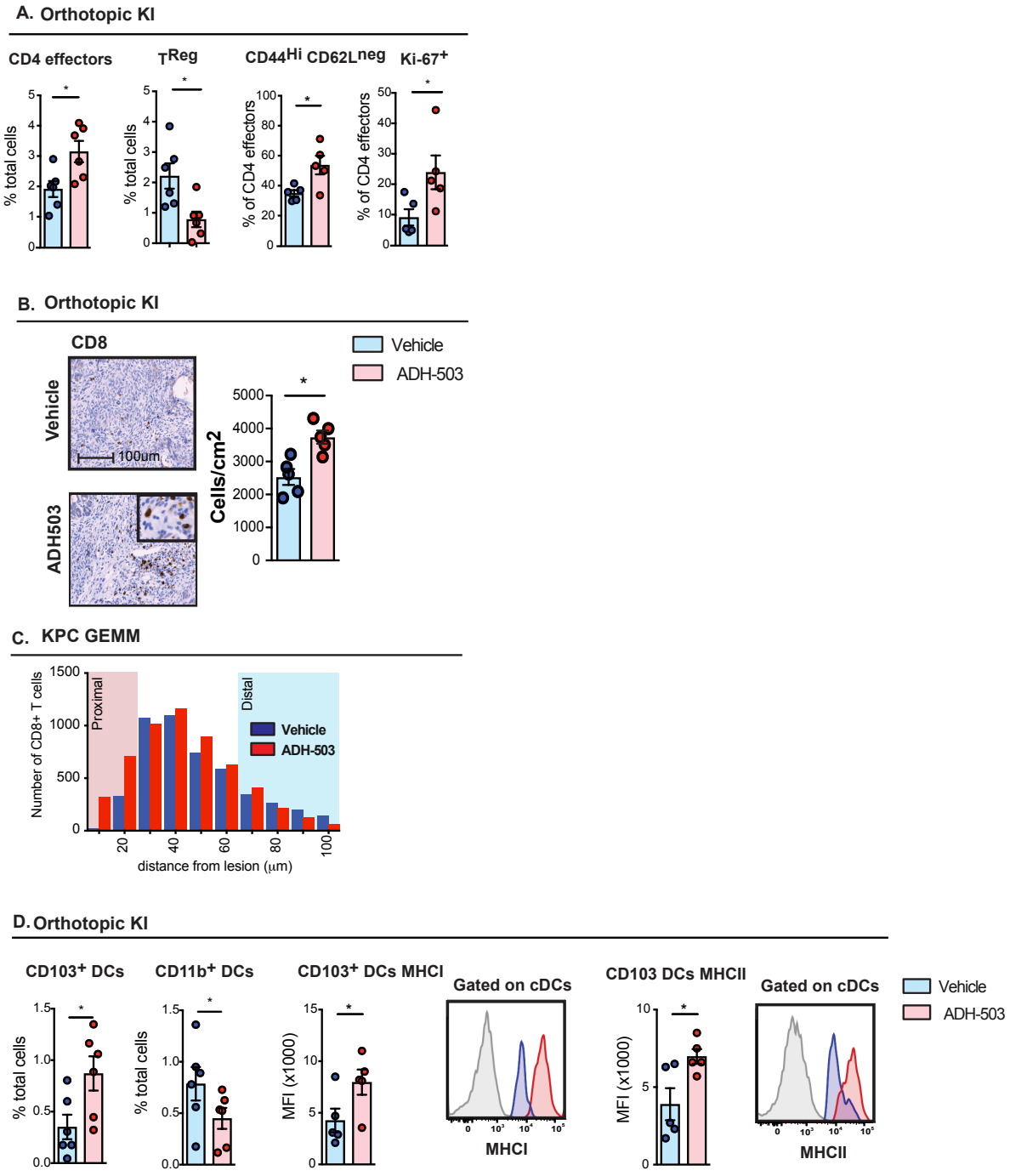
A. Orthotopic KI
CD4 effectors
TReg
CD44Hi CD62Lneg
Ki-67+
% total cells
% of CD4 effectors
B. Orthotopic KI
CD8
Vehicle
ADH-503
100um
Cells/cm2
C. KPC GEMM
Number of CD8+ T cells
Proximal
Distal
Vehicle
ADH-503
distance from lesion (μm)
D. Orthotopic KI
CD103+ DCs
CD11b+ DCs
CD103+ DCs MHCI
Gated on cDCs
MHCI
CD103 DCs MHCII
Gated on cDCs
MHCII
MFI (x1000)

Supplementary Fig. 4: CD11b-agonism stimulates T cell and cDC1 infiltration and function.

A) Flow cytometry of tumor-infiltrating $CD4^+$ $FOXP3^+$ regulatory T cells, and $FOXP3^-$ T effectors in orthotopic KI PDAC tissues from mice treated 12 days with ADH-503 or vehicle. Graphs show the mean T cell frequency and subsets of CD4+ effectors marked by $CD44^{Hi}CD62L^{Low}$ or Ki-67 (n=5-6/group).

B) Representative IHC staining images of $CD8^+$ cells in KI tumor tissues from mice treated with vehicle or ADH-503 for 14 days (10X images). Quantification is shown in bar graphs (n=5/group).

C) The histogram shows the relative $CD8a^+$ cell number binned by cellular distances from $CK19^+$ cells. Analysis was done on tissue from KPC GEMMs treated with vehicle or ADH-503 (n=6/group).

D) Frequency of CD11b+ and $CD103^+$ DCs and expression of MHC-I and MHC-II expression in CD103+ cDCs in KI PDAC tissues from mice treated with vehicle or ADH-503 for 12 days. Mean cell percentages and GEO-MFI data are shown. (n=4-6)

Graphs show the mean ± standard error; * denotes $P < 0.05$ by two-sided *t* test or Mann-Whitney test, depending on the data distribution. All flow cytometry data are representative of 2–3 independent in vivo experiments.

Figure S5

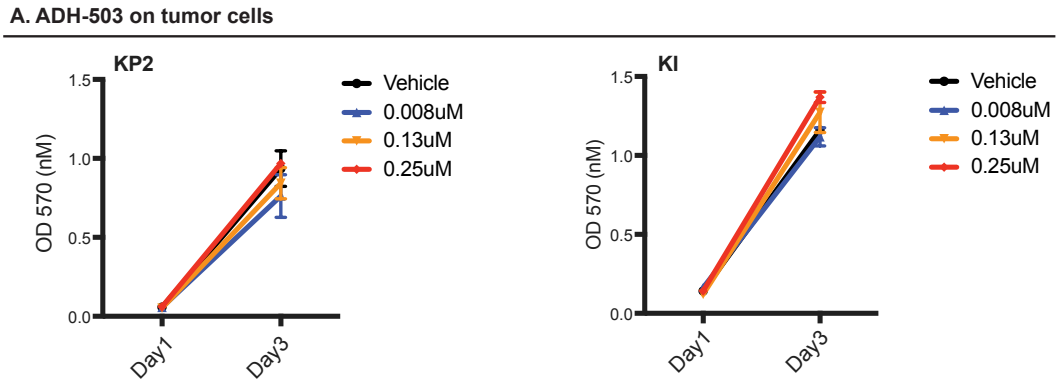
A. ADH-503 on tumor cells
KP2
OD 570 (nM)
1.5
1.0
0.5
0.0
Day1
Day3
Vehicle
0.008uM
0.13uM
0.25uM
KI
OD 570 (nM)
1.5
1.0
0.5
0.0
Day1
Day3
Vehicle
0.008uM
0.13uM
0.25uM

Supplementary Fig. 5: ADH-503 direct effects on PDAC cells

KP2 and KI tumor cells were grown on collagen and cell proliferation was measured by MTT assay in the presence of vehicle or ADH-503. n=3 assays/condition

Figure S6

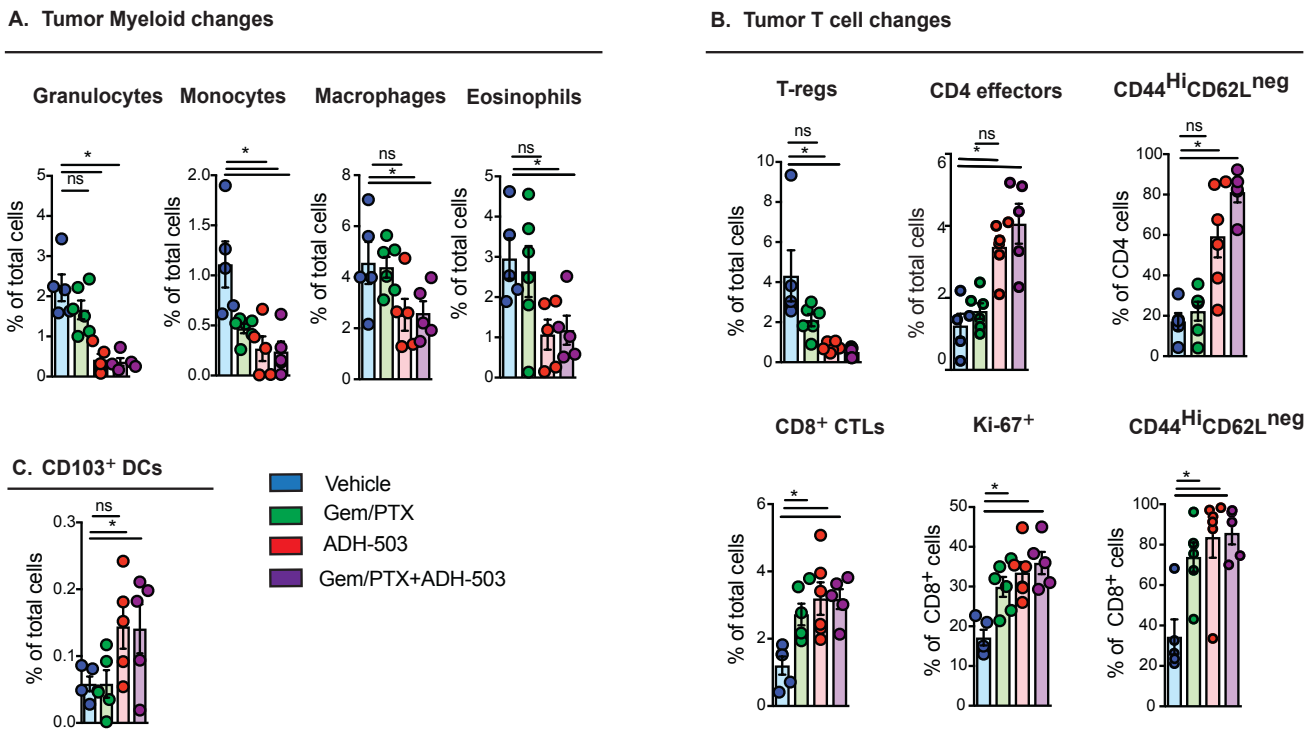
A. Tumor Myeloid changes
Granulocytes
Monocytes
Macrophages
Eosinophils
% of total cells
B. Tumor T cell changes
T-regs
CD4 effectors
CD44Hi CD62Lneg
% of CD4 cells
CD8+ CTLs
Ki-67+
% of CD8+ cells
C. CD103+ DCs
Vehicle
Gem/PTX
ADH-503
Gem/PTX+ADH-503
ns
*

Supplementary Fig. 6: CD11b agonism in combination with chemotherapy.

A) Flow cytometric frequencies of tumor infiltrating granulocyte, monocyte, eosinophil and macrophage and cDC1s in orthotopic KrasINK model, after 12 days of treatment with ADH-503 or vehicle +/- GEM/PTX (n=5/ group).

B-C) Flow cytometric frequencies of tumor infiltrating $CD4^+$ and $CD8^+$ T cell and their Ki67+ or CD44+CD62L- fractions in tissue from (A). (n=5/ group)

C) Flow cytometric frequencies of tumor infiltrating cDC1s. (n=5/ group)

Graphs show the mean ± standard error; * denotes $P < 0.05$ by two-sided *t* test.

Figure S7

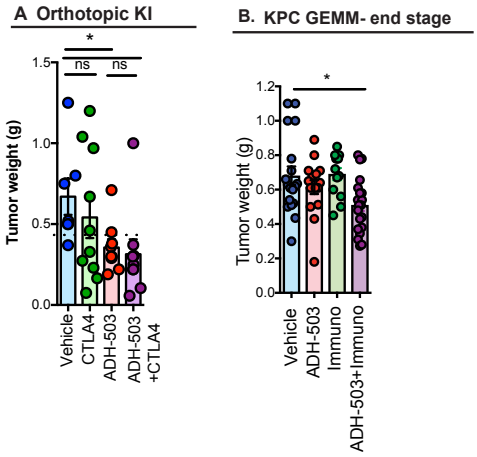
A Orthotopic KI
*
ns
ns
Tumor weight (g)
1.5
1.0
0.5
0.0
Vehicle
CTLA4
ADH-503
ADH-503 +CTLA4
B. KPC GEMM- end stage
*
Tumor weight (g)
1.2
1.0
0.8
0.6
0.4
0.2
0.0
Vehicle
ADH-503
Immuno
ADH-503+Immuno

Supplementary Fig. 7: Tumor wet weights

A) Tumor burden 14 days after treatment with vehicle or ADH-503 ± anti-CTLA4 in orthotopic KI PDAC models (n = 7-10/group).

B) Tumor burden from end-stage KPC mice from survival analysis in Figure 7E. “Immuno” is treatment with gemcitabine + anti-PD1 + anti-CTLA4. Mice were enrolled in the study when tumors were greater than 0.4 cm in diameter (n = 10–15/group).

Graphs show the mean ± standard error; * denotes $P < 0.05$ by two-sided *t* test.

Table S1. Mouse Antibodies for Flow Cytometry and FACS

Antigen	Clone	Fluorophore	Source
B220	RA3-6B2	APC	BioLegend
CD3	145-2C11	APC, PerCP-Cy5.5, BV711	eBioscience, BD Horizon
CD11b	M1/70	Alexa700, PE-Cy7	eBioscience
CD16/CD32	93	Unconjugated	eBioscience
CD19	eBio1D3	APC	eBioscience
	6D5	APC-Cy7	eBioscience
CD40	1C10	PE-Cy5	eBioscience
CD45	30-F11	PE-Cy7, APC-Cy7	eBioscience
CD80	16-10A1	PE-Cy5	eBioscience
CD86	GL1	PE-Cy5	eBioscience
F4/80	BM8	PE-Cy5, PE	eBioscience
MHCI	34-1-2S	PE	eBioscience
MHCII	M5/114.15.2	eFluor450, APC-Cy7	eBioscience
PD1	J43	PE	eBioscience
Ly6C	HK1.4	PerCP-Cy5.5, Alexa488	eBioscience
Ly6G	1A8	PE	eBioscience
		APC	BioLegend
Ki67	SoADH-5035	APC	eBioscience
CD4	RM4-4	FITC	eBioscience
CD8a	53-6.7	BUV-395	BD Horizon
CD44	IM7	eFluor 450	eBioscience
CD62L	MEL-14	BV-605	Biolegend
Tim3 (CD366)	RMT3-23	PE-Cy7	eBioscience
FoxP3	FJK-16s	PE-Cy5	eBioscience
Eomesodermin	Dan11mag	PE-Cy7	eBioscience
CD24	30-F1	FITC	eBioscience
CD103	2E7	BV-510	Biolegend
CD11c	N418	APC	eBioscience
PDL1	MIH5	PE	eBioscience
NK1.1	PK136	BV421	BD Horizon
CD22	OX-97	FITC	Biolegend
CD49b	DX5	APC	eBioscience
γδTCR	eBioGL3	PE	eBioscience

Table S2. Tissue IHC and IF Antibodies

Antigen	Clone	Species	Source
CD68 (1:2000)	Polyclonal Ab125212	Rabbit anti-mouse	Abcam
SMA (1:200)	ab5694	Rabbit anti-mouse	Abcam
FAP (1:200)	Polyclonal 2586813	Rabbit anti-mouse	Millipore
Gr-1-biotin (1:1000)	ab25680	Rat-biotin anti-mouse	Abcam
CD8 (1:1000)	4SM16	Rat anti-mouse	eBiosciences
CD8a-biotin	53-6.7	Rat anti-mouse	eBiosciences
Pan-Keratin-488 conjugate	C11	Mouse	Cell Signaling
Ki67 (1:500)	Polyclonal Ab15580	Rabbit anti-mouse	Abcam
CD11b (1:100)	NP57	Mouse anti-human	Santa Cruz Biotech
CD14 (1:100)	ab10628	Rabbit anti-human	Abcam
CD15 (1:100)	ab754	Mouse anti-human	Abcam
Cleaved Caspase-3 (1:200)	ASP175	Rabbit anti-mouse	Cell Signaling
CK19 (1:1000)	D4G2	Rabbit anti-human	Cell Signaling

Table S3. Antibodies for CyTOF Staining

Target	Clone	Manufacturer	Catalog N
CD45	HI30	Fluidigm	3089003B
CD3	UCHT1	BioLegend	300402_B
CD19	HIB19	Fluidigm	3142001B
CD81	5A6	Fluidigm	3145007B
CD64	10.1	Fluidigm	3146006B
CD20	2H7	Fluidigm	3147001B
CD16	3G8	Fluidigm	3148004B
CD34	581	Fluidigm	3149013B
CD86	IT2.2	Fluidigm	3150020B
CD115	12-3A3-1B10	Biolegend	B201393
CD1c	L161	Biolegend	331501
CD192 (CCR2)	K036C2	Fluidigm	3153023B
CD163	GHI/61	Fluidigm	3154007B
CD82	ASL-24	Fluidigm	3158025B
CD11c	Bu15	Fluidigm	3159001B
CD14	M5E2	Fluidigm	3160001B
Ki-67	B56	Fluidigm	3161007B
CD80 (B7-1)	2D10.4	Fluidigm	3162010B
pcna	PC10	Abcam	Ab29
CD15 (SSEA-1)	W6D3	Fluidigm	3164001B
CD40	5C3	Fluidigm	3165005B
CD24	ML5	Fluidigm	3166007B
CD38	HIT2	Fluidigm	3167001B
CD206 (MMR)	15-2	Fluidigm	3168008B
CD32	FUN-2	Fluidigm	3169020B
CD54	HA58	Fluidigm	3170014B
CD68	Y1/82A	Fluidigm	3171011B
CX3CR1	2A9-1	Fluidigm	3172017B
CD141	1A4	Fluidigm	3173002B
HLA-DR	L243	Fluidigm	3174001B
CXCR4	12G5	Fluidigm	3175001B
CD56	NCAM16.2	Fluidigm	3176008B
CD11b (Mac-1)	ICRF44	Fluidigm	3209003B